DISCRETE, CONTINUOUS, AND VIRTUAL MODES IN UNDERWATER SOUND PROPAGATION

TEXAS UNIVERSITY AT AUSTIN

26 AUGUST 1976

THE UNIVERSITY OF TEXAS AT AUSTIN

ARL-TR-76-40
26 August 1976

Copy No. 43

DISCRETE, CONTINUOUS, AND VIRTUAL MODES IN UNDERWATER SOUND PROPAGATION

A. O. Williams Jr.
Brown University, Providence, Rhode Island,
and Applied Research Laboratories,
The University of Texas at Austin

NAVAL ELECTRONIC SYSTEMS COMMAND
Contract N00039-76-C-0081

UNCLASSIFIED
SECURITY CLASSIFICATION OF THIS PAGE (When Data Entered)

REPORT DOCUMENTATION PAGE

READ INSTRUCTIONS BEFORE COMPLETING FORM

1. REPORT NUMBER: ARL-TR-76-40
2. GOVT ACCESSION NO.:
3. RECIPIENT'S CATALOG NUMBER:

4. TITLE (and Subtitle): Discrete, Continuous, and Virtual Modes in Underwater Sound Propagation
5. TYPE OF REPORT & PERIOD COVERED: Technical Report
6. PERFORMING ORG. REPORT NUMBER:

7. AUTHOR(s): A. O. Williams, Jr.
8. CONTRACT OR GRANT NUMBER(s): N00039-76-C-0081

9. PERFORMING ORGANIZATION NAME AND ADDRESS:
Applied Research Laboratories
The University of Texas at Austin
Austin, Texas 78712
10. PROGRAM ELEMENT, PROJECT, TASK AREA & WORK UNIT NUMBERS:

11. CONTROLLING OFFICE NAME AND ADDRESS:
Naval Electronic Systems Command
Department of the Navy
Washington, DC 20360
12. REPORT DATE: 26 August 1976
13. NUMBER OF PAGES: 51

14. MONITORING AGENCY NAME & ADDRESS (if different from Controlling Office):
15. SECURITY CLASS. (of this report): Unclassified
15a. DECLASSIFICATION/DOWNGRADING SCHEDULE:

16. DISTRIBUTION STATEMENT (of this Report):
Approved for public release;
distribution unlimited

17. DISTRIBUTION STATEMENT (of the abstract entered in Block 20, if different from Report):

18. SUPPLEMENTARY NOTES:

19. KEY WORDS (Continue on reverse side if necessary and identify by block number):
underwater sound propagation
normal modes
branch line integral
virtual modes

20. ABSTRACT (Continue on reverse side if necessary and identify by block number):
Adopting two physical postulates and using only the language of eigenfunctions and eigenvalues, we express the underwater sound field of a harmonic point source as a sum over orthonormal discrete modes plus an integral over a continuous set of normal modes. Restrictions are constant water depth, no absorption, parameters varying only with depth, and bottom material treated as a fluid. For the Pekeris case, orthogonality of the continuous modes is demonstrated (throughout this (U)

DD FORM 1 JAN 73 1473 EDITION OF 1 NOV 65 IS OBSOLETE

UNCLASSIFIED
SECURITY CLASSIFICATION OF THIS PAGE (When Data Entered)

20. Abstract (contd.)

report, orthonormality is with respect to a weighting function, the material density), and the integral over continuous modes is proved identical to the branch line integral (BLI) of Ewing, Jardetzky, and Press. We show that farfield contributions to BLI are practically negligible except for contributions from narrow "spikes" or resonances of the integrand. Conditions for existence of resonances are stated. Resonances lead to virtual modes (discussed by Labianca and by Tindle and Guthrie) that decay faster with range than a discrete mode does. Some computer results by Stickler are examined semianalytically in terms of discrete and virtual modes; agreement is fairly good. We find that BLI also has a "pseudoresonance", yielding a virtual mode, when a discrete mode is near cutoff. Comments on Bartberger's method of improper modes are added. (U)

ARL-TR-76-40
26 August 1976

DISCRETE, CONTINUOUS, AND VIRTUAL MODES IN UNDERWATER SOUND PROPAGATION

A. O. Williams, Jr.
Brown University, Providence, Rhode Island,
and Applied Research Laboratories,
The University of Texas at Austin

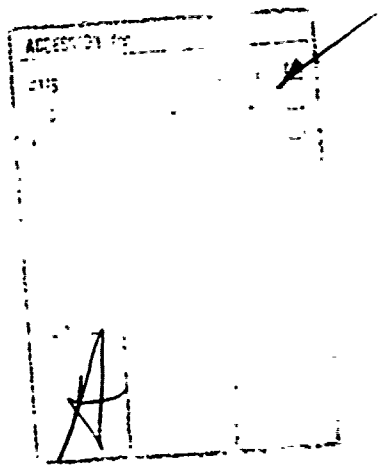

NAVAL ELECTRONIC SYSTEMS COMMAND
Contract N00039-76-C-0081

APPLIED RESEARCH LABORATORIES
THE UNIVERSITY OF TEXAS AT AUSTIN
AUSTIN, TEXAS 78712

ABSTRACT

Adopting two physical postulates and using only the language of eigenfunctions and eigenvalues, we express the underwater sound field of a harmonic point source as a sum over orthonormal discrete modes plus an integral over a continuous set of normal modes. Restrictions are constant water depth, no absorption, parameters varying only with depth, and bottom material treated as a fluid. For the Pekeris case, orthogonality of the continuous modes is demonstrated (throughout this report, orthonormality is with respect to a weighting function, the material density), and the integral over continuous modes is proved identical to the branch line integral (BLI) of Ewing, Jardetzky, and Press. We show that farfield contributions to BLI are practically negligible except for contributions from narrow "spikes" or resonances of the integrand. Conditions for existence of resonances are stated. Resonances lead to virtual modes (discussed by Labianca and by Tindle and Guthrie) that decay faster with range than a discrete mode does. Some computer results by Stickler are examined semianalytically in terms of discrete and virtual modes; agreement is fairly good. We find that BLI also has a "pseudoresonance", yielding a virtual mode, when a discrete mode is near cutoff. Comments on Bartberger's method of improper modes are added.

TABLE OF CONTENTS

INTRODUCTION

We consider the propagation of cw single frequency sound in a medium that comprises a water layer of constant depth H and a bottom half-space, treated as a fluid. The sound speed c varies only with depth z, which is measured vertically downward from z=0 at the water surface. The material density ρ also may vary with z, but at most it varies via finite discontinuities at one or more values of z. An omnidirectional point source of angular frequency ω is at depth z=d on the z axis. Horizontal range r is measured from the z axis.

The acoustic velocity potential $\Phi(r,z)$--a time factor $\exp(+i\omega t)$ having been suppressed--can be represented as a sum over a finite set of discrete normal modes plus another contribution expressible as either a branch line integral (BLI) or an integral over a continuous set of normal modes. If H/λ (λ is the acoustic wavelength) is small enough, the discrete set is empty. If certain artificial boundary conditions are given, the continuous set can be empty but then the discrete set is countably infinite.

In the sections that follow, we first discuss the normal modes of the medium in the absence of any source, using the language of eigenfunctions and eigenvalues. Throughout the report, effects of absorption are neglected as are all other dissipative effects, e.g., the slight acoustic leakage through the water surface to the air above. We "connect" these modes to the point source described above and show, for the special case of a Pekeris problem, that the sum of discrete modes is identical to that found by Pekeris,[1] Ewing, Jardetzky, and Press (EJP),[2] and others. Continuing with the Pekeris problem, we find the continuous modes, normalize them, prove that they are orthogonal, and demonstrate that the integral over all continuous modes is identical to the BLI found by EJP.[2] This result adds support to an

argument by Stickler[3] that the EJP branch line integral is to be preferred over that of Pekeris.

Next, the EJP integral is examined. It turns out that for sufficiently large r, i.e., in the farfield, the integral practically vanishes, unless in some part or parts of the range of integration the integrand displays large and narrow peaks or troughs. The effect of such a "spike" is much the same as that of an extra discrete mode being introduced, which suggests that Bartberger's "improper modes"[4,5] can be explained thus. Labianca discussed a closely similar problem[6] and, following quantum mechanical nomenclature, referred to the "extra modes" as virtual modes. We use his terminology and test the effects of such modes against computer results published by Stickler.[3] Reasonable agreement is found.

It should be noted that just after this manuscript was drafted a preprint arrived from two New Zealand scientists.[7] They applied Labianca's method to the kind of problem discussed here and--still in accord with quantum mechanics--designated the "spikes" that lead to virtual modes as resonances, a term that we also adopt. There is considerable but far from complete overlap of Ref. 7 and our analysis.

I. Two Postulates Concerning Normal Modes

The term normal mode can have various meanings. It may mean a pattern of motion characteristic of a specified medium (which is our meaning here) or a pattern characteristic of a specified medium with a specified source in it. There are many other examples. (See a discussion by Biot and Tolstoy.[8]) We might use the term "exotic mode" (in no pejorative sense) to mean one that appears to be a valid mathematical solution of the particular problem. Yet at first glance and often, too, at second glance, the exotic mode has surprising behavior, e.g., it diverges to infinite amplitude as $z \to \infty$. We claim no proficiency in that powerful method of solution, integration in the

complex plane, but the method does seem prone to yield exotic as well as "familiar" modes.[3-5] The following two postulates appear to be relevant.

Postulate 1. In the propagation problem outlined in the Introduction, the mathematical functions $c(z)$ and $\rho(z)$ purporting to represent the behavior of sound speed and density must be physically reasonable. Finite discontinuities are allowable as good approximations to rapid continuous changes, but $c(z)$ and $\rho(z)$ cannot vanish, have singularities, or turn imaginary at any depth z where the sound field is nonnegligible.[9]

The special case in which $c(z)\to\infty$ as $z\to\infty$ may be open to debate (or perhaps it is covered by Ref. 9), but we note that the resulting bottom reflection coefficient appears to have unit magnitude for all angles of incidence. A more serious example of misbehavior is the pseudolinear positive gradient of sound speed: $c(z)=c_o[1-\beta(z-z_o)]^{-1/2}$, $\beta>0$, $z\geq z_o$. At certain angles of incidence, this $c(z)$ leads to bottom reflection coefficients of magnitude exceeding unity.[10] Some of Bartberger's difficulties with exotic modes apparently stem from the use of this equation in depths at which it has become unphysical.

Postulate 2. Each normal mode of a medium represents a conceivable physical pattern of behavior. The set of all such modes--discrete plus continuous--must be normalizable, complete, and closed on the range $0\leq z\leq\infty$. (The additional property of orthogonality is extremely convenient, but in physical problems it probably exists automatically or is achievable.)

The preceding statements require that each mode, separately, must satisfy the wave equation and all pertinent acoustic boundary conditions and must be quadratically integrable. The last requirement appears to rule out Bartberger's "improper" or "bad" modes,[4,5] which diverge at $z=\infty$. However, we must not dodge the fact that inclusion of these

modes often affects the total solution in ways confirmed by different methods of evaluation. This matter is discussed later.

Another intent of this postulate is to rule out a priori imposition of additional properties on any single mode, e.g., that it must be a traveling wave or a standing wave. Only the totality of all modes determines the behavior of the sound field.

II. Eigenfunctions and Eigenvalues of Our Problem

For a single frequency point source, the acoustic velocity potential Φ is governed by the inhomogeneous Helmholtz equation

$$\nabla^2\Phi + k^2(z)\Phi = -\delta(\vec{r}-\vec{r}_o) \quad , \tag{1}$$

$$k^2(z) = \frac{\omega^2}{c^2(z)} \quad , \quad 0 \leq z \leq \infty \quad . \tag{2}$$

The right-hand side of Eq. 1, a three-dimensional delta function, corresponds to having an omnidirectional point source at $\vec{r}_o$. Since we assume cylindrical symmetry about the z axis, Eq. 1 reduces to

$$r^{-1}\left(\frac{\partial}{\partial r}\right)r\left(\frac{\partial\Phi}{\partial r}\right) + \frac{\partial^2\Phi}{\partial z^2} + k^2(z)\Phi = -\frac{\delta(r)\delta(z-d)}{2\pi r} \quad . \tag{3}$$

The homogeneous equation corresponding to Eq. 3 is separable. We take $\Phi(r,z)=R(r)Z(z)$ and proceed in the usual way, with separation constant K^2. The z equation is

$$\frac{d^2Z}{dz^2} + [k^2(z)-K^2]\,Z(z) = 0 \quad . \tag{4}$$

Each acceptable solution Z must be normalizable over $0 \leq z \leq \infty$ and must obey all pertinent acoustic boundary conditions at all finite depths. These conditions are (1) continuity of acoustic pressure and therefore of ρZ and (2) continuity of normal particle velocity and therefore of dZ/dz. At the water surface the sole condition is that $Z=0$. Apart from the requirement of normalizability, we postpone any comment about the radiation condition at infinity. A pertinent fact of geophysics is that $c(z)$ and $\rho(z)$ will always exceed their maximum values in the water layer, at and below a sufficiently great depth in the bottom.

It follows that Eq. 4 must be solved as an eigenvalue problem. The set of acceptable Z's includes a subset (possibly empty) with a finite number of discrete Z_n's, marked by discrete values k_n^2 of the separation constant K^2. The rest of the set is made up of the continuous Z's, in which adjacent Z's and their values of K^2 differ infinitesimally. For them, we write K^2 as k^2.

As Biot and Tolstoy[8] have shown, orthonormality for any acceptable Z's must be with respect to a weighting function $\rho(z)$. That is, if K and K' correspond to two values of K^2, the integral to be treated is

$$I(K,K') = \int_0^\infty \rho(z)\, Z_K(z) Z_{K'}(z) dz = \delta_{K,K'} \text{ or } \delta(K-K') \quad . \qquad (5)$$

Following postulate 2 of Section I, we assume that the whole set $\{Z(k,z)\}$ is complete (in practical terms this assumption means that we have taken pains to find all acceptable Z's) and is also closed. Completeness allows writing $\varphi(r,z)$ as

$$\varphi(r,z) = \mathbf{S}_K A(K,r) Z(K,r) \quad . \qquad (6)$$

Here $\mathbf{S}$ implies, in effect, a Stieltjes integral--a sum over discrete Z_n's and an integral over continuous Z's. Closure of the set is expressed by

$$\mathbf{S}_K Z(K,z)Z(K,z') = \delta(z-z') \quad . \tag{7}$$

In Eqs. 6 and 7, it is assumed that the Z's have already been normalized. Taking z'=d, the source depth and substituting Eqs. 6 and 7 in Eq. 5 leads to

$$\mathbf{S}_K Z(K,z) \left\{ \frac{1}{r} \frac{d}{dr} \left[r \frac{dA(K,r)}{dr} \right] + K^2 A + \frac{\delta(r) Z(K,d)}{2\pi r} \right\} = 0 \quad . \tag{8}$$

It follows that {...} vanishes identically. The resulting solution is

$$A(K,r) = \left(\frac{i}{4}\right) Z(K,d) H_o^{(2)}(Kr) \quad , \tag{9}$$

in which the proper Hankel function has been chosen to ensure an outgoing cylindrical wave. The final expression for φ is

$$\varphi(r,z) = iC \mathbf{S}_K Z(K,d)Z(K,z)H_o^{(2)}(Kr) \quad . \tag{10}$$

The arbitrary constant C, allowed because this problem is linear, has subsumed the factor 1/4 of Eq. 9. The Z's in Eqs. 7 through 10 are normalized.

Orthogonality is readily demonstrated for the discrete modes, provided that $\rho(z)$ is piecewise constant. (If this behavior is violated, the acoustic wave equation must be reexamined; the complications resemble those in nonlinear acoustics.) We treat the case of a single discontinuity in $\rho(z)$, at z=H; generalizing to any finite number of discontinuities is simple. Writing Eq. 4 for Z_n and K_n^2, we

multiply through by Z_m, repeat the process with n and m interchanged, subtract one equation from the other, and obtain (with primes for d/dz)

$$Z_m Z_n'' - Z_n Z_m'' = \frac{d}{dz}\left(Z_m Z_n' - Z_n Z_m'\right) = (k_n^2 - k_m^2) Z_m Z_n \quad . \tag{11}$$

After multiplying through by $\rho(z)$, we integrate both sides, from z=0 to H and from H to ∞:

$$\rho_w \left[Z_m Z_n' - Z_n Z_m'\right]_0^H + \rho_b \left[Z_m Z_n' - Z_n Z_m'\right]_H^\infty = (k_n^2 - k_m^2) \int_0^\infty \rho(z) Z_m Z_n dz \quad . \tag{12}$$

The Z's vanish at the pressure-release surface, z=0. They also vanish at $z=\infty$ if postulate 2 and the comments about c(z) at great depth (see the paragraph following Eq. 4) are accepted. The left-hand side of Eq. 12 becomes

$$[\rho_w Z_{mw}(H) Z'_{nw}(H) - \rho_b Z_{mb}(H) Z'_{nb}(H)] - [\ldots] \quad . \tag{13}$$

Here subscripts w and b mean "in the water," "in the bottom," and the second [ ] is the same as the first, with n and m interchanged. The acoustic conditions, or the continuity of ρZ and of Z' at H, ensure that all of expression 13 vanishes, and hence Z_m and Z_n are orthogonal for $k_n^2 \neq k_m^2$. The proof just given does not imply that orthogonality must fail when $\rho(z)$ varies continuously.

Still considering only discrete modes, we apply Eq. 10 to the Pekeris problem.[1] c(z) and $\rho(z)$ are piecewise constant, being c_w, ρ_w in the water and $c_b > c_w$, $\rho_b > \rho_w$ in the bottom. The acceptable unnormalized Z's are evident from Eq. 4 (with $K^2 = k_n^2$) and postulate 2:

$$Z_n = \sin(\beta_1 z), \quad \beta_1 = +\left(k_w^2 - k_n^2\right)^{1/2} \quad , \quad 0 \leq z < H \quad , \qquad (14)$$

and

$$\left.\begin{aligned} Z_n &= \text{const.} \times \exp(-\beta_2' z) = \gamma \exp[-\beta_2'(z-H)], \quad z > H \\ \beta_2' &= +\left(k_n^2 - k_b^2\right)^{1/2} \quad . \end{aligned}\right\} \qquad (15)$$

The behavior of k_n^2 assumed in these equations is easily traced. It is a fundamental property of the eigenvalue problem associated with Eq. 4 that the sets $\{Z_n\}$ and $\{k_n^2\}$ can be so ordered, with $n=1,2,3,\ldots$, that Z_{n+1} in $0<z<\infty$ has one more zero than does Z_n. Since Z_n of Eq. 15 has no zero in this range, it is clear that β_1 (Eq. 14) must rise with n and, therefore, that k_n^2 must fall. However, k_n^2 cannot be less than k_b^2 or else Eq. 15 must have a complex exponential, and then the acoustic conditions at z=H cannot be satisfied. (If absorption is present, k_n^2 may somewhat exceed k_b^2.)

By applying these conditions at z=H, we obtain

$$\tan(\beta_1 H) = -\left(\frac{\rho_b}{\rho_w}\right)\left(\frac{\beta_1}{\beta_2'}\right) \quad , \qquad (16)$$

which is the eigenvalue equation for the numerical determination of k_n^2. We also find, with the help of Eq. 16, that

$$\gamma^2 = \left(\frac{\rho_w}{\rho_b}\right)^2 \sin^2(\beta_1 H) \quad . \qquad (17)$$

The Z_n's of Eqs. 14 and 15 are normalized, as in Eq. 5, to the form $N_n Z_n(z)$ by direct integration. The result is

$$N_n = \left(\frac{2\beta_1}{\rho_w}\right)^{1/2}\left[\beta_1 H - \sin(\beta_1 H)\cos(\beta_1 H) - \left(\frac{\rho_w}{\rho_b}\right)^2 \sin^2(\beta_1 H)\tan(\beta_1 H)\right]^{-1/2} . \quad (18)$$

Considering only $0<d<H$, we substitute Eqs. 14 and 18 in Eq. 10, and then repeat with Eqs. 15, 17, and 18. The two results are identical respectively to Eqs. A48 and A50 of Ref. 1, if we take $C=-\pi\rho_w$. They are also identical to the corresponding equations of EJP.[2] There is nothing novel about this, for no one has ever doubted such agreement; our main point in this exercise is to establish the proper value of C for later use. There is, however, a touch of historical irony. Temporarily adopting the language of eigenfunctions (see Ref. 1, pp. 53-55), Pekeris expressed concern over the failure of these functions to be orthogonal unless $\rho_w=\rho_b$. The cause was overlooking the need of a weighting function (Eq. 5). The irony was that his method of integration in the complex plane had automatically produced the effect of proper orthonormal eigenfunctions in the sense of Eq. 5.

We observe that Eq. 16 allows no discrete mode unless $\beta_1 H>\pi/2$ and that, in conjunction with Eq. 15, it allows at most a finite number of modes.

III. Continuous Modes of the Pekeris Problem

Through the rest of this discussion we consider only the Pekeris problem, without absorption. For the continuous modes, Eq. 4 still holds. We now write $Z(k,z)$ and $K=k$ instead of k_n, with k a continuous variable. Equation 14 also holds with these changes of notation, and the expression for β_1 is unchanged. However, Eq. 15 is different because now $k^2<k_b^2$ (see the remarks immediately following Eq. 15). Acceptable unnormalized Z's in the bottom are

$$Z(k,z) = \mu \sin(\beta_2 z+\nu) \quad , \quad \beta_2 = +\left(k_b^2-k^2\right)^{1/2} \quad , \quad z > H \quad , \quad (19)$$

with μ and ν being two functions of k yet to be determined. (The only other conceivable form for Z would be a complex exponential, but then the acoustic conditions at z=H could not be met.) After writing those conditions, we obtain two equations from them. One is the eigenvalue equation,

$$\left(\frac{\rho_w}{\beta_1}\right)\tan(\beta_1 H) = \left(\frac{\rho_b}{\beta_2}\right)\tan(\beta_2 H+\nu) \quad , \tag{20}$$

which--thanks to the leeway afforded by the extra constant ν--can be satisfied for any $k^2<k_b^2$. The other equation yields μ^2:

$$\mu^2 = \left(\frac{\beta_1}{\beta_2}\right)^2 \cos^2(\beta_1 H) + \left(\frac{\rho_w}{\rho_b}\right)^2 \sin^2(\beta_1 H) \quad . \tag{21}$$

We normalize Z(k,z) to obtain $N_k Z$, as in Eq. 5, by the method of "box normalization." That is, the integral from H to ∞ is carried out from H to (H+L)>>H, and eventually L is allowed to increase indefinitely. The result is

$$N_k^{-2} = \rho_w \int_0^H \sin^2(\beta_1 z)dz + \rho_b \mu^2 \int_H^{H+L} \sin^2(\beta_2 z+\nu)dz \tag{22}$$

$$= \text{const.} \times L^0 + \left(\frac{\rho_b \mu^2}{2\beta_2}\right)\left[\beta_2 z + \nu - \frac{1}{2}\sin(2\beta_2 z+2\nu)\right]_H^{H+L} \quad . \tag{23}$$

The sine term is also const. $\times L^0$, ν drops out, and the outcome is

$$N_k^2 = \left(\frac{2}{\rho_b \mu^2 L}\right) \quad . \tag{24}$$

To demonstrate orthogonality in the sense of Eq. 5, we let β_1, β_2,ν correspond to one value of k and β_1',β_2',ν' to another value, k'. (This β_2' is not the same one that is used in Eq. 15.) Temporarily, we drop subscript 2 from β_2,β_2', since β_1 does not appear anywhere in this calculation. Also we express β and β' as

$$\beta = \frac{m\pi}{L} \quad , \quad \beta' = \frac{m'\pi}{L} \quad , \tag{25}$$

where

$$m \neq m' \quad ; \quad m,m' = 0,1,2,\ldots, \quad . \tag{26}$$

This step restricts β and β' to discrete changes. However, the smallest change is π/L, which approaches a differential quantity when L is allowed to increase without limit.

We can now make use of the method in Eqs. 11 through 13 for arbitrarily large but finite L because the continuous modes have been rendered discrete by Eqs. 25 and 26. The only change is that, in Eq. 12, the upper limit ∞ is replaced by H+L on both sides of the equation. Consequently, some extra terms appear in the left-hand side of Eq. 12:

$$\rho_b[Z_m(H+L)\, Z_n'(H+L) - Z_n(H+L)\, Z_m'(H+L)] = N_k N_k' \mu\mu' \rho_b$$
$$\times \left\{\beta' \sin[\beta(H+L)+\nu] \cos[\beta'(H+L)+\nu'] - \beta \cos[\beta(H+L)+\nu] \sin[\beta'(H+L)+\nu']\right\} \quad . \tag{27}$$

The right-hand side of Eq. 27 results from Eq. 19. With the use of Eq. 24, the term $N_k \ldots \rho_b$ in Eq. 27 becomes simply 2/L. We remove βL and $\beta' L$ from within { } by invoking Eq. 25 and noting that

$$\sin(m\pi+\theta) = (-)^m \sin\theta \quad ; \quad \cos(m\pi+\theta) = (-)^m \cos\theta \quad . \tag{28}$$

The outcome is that the right-hand side of Eq. 27--the extra terms in Eq. 12--is

$$\frac{2(-)^{m+m'}}{L} \times [\beta' \sin(\beta H+\nu) \cos(\beta' H+\nu') - \beta \cos(\beta H+\nu) \sin(\beta' H+\nu')] \quad . \quad (29)$$

For any given pair of modes denoted by β and β', this expression vanishes as $L \to \infty$. Simultaneously, the upper limit H+L on the integral in Eq. 12 once more becomes ∞. Therefore the continuous modes are mutually orthogonal. The orthogonality of any discrete and any continuous mode can be proved similarly.

If postulates 1 and 2 are observed, finding the normal modes for more complicated cases would differ mainly in detail. Equation 10 remains correct, and for the discrete modes, so do the steps in Eqs. 11 through 13. Normalizing these modes would be accomplished by direct integration. The corresponding treatment of continuous modes could proceed via box normalization. However, the calculations will be more difficult than they are for a Pekeris case.

IV. Equation 10 and the Branch Line Integral

The continuous-mode part, φ_c, of φ in Eq. 10, can now be written as follows:

$$\varphi_c(r,z) = iC \sum_m N_k^2 Z(k,d) Z(k,z) H_o^{(2)}(kr) \quad , \quad (30)$$

with the unnormalized Z's from Eqs. 14 and 19 as pertinent. (Thanks to Eq. 25, β_1, β_2, k, and all functions of them are determined by the integer m; hence, summation is correct). As $L \to \infty$, the changes in quantities corresponding to $\Delta m = \pm 1$ are essentially infinitesimal and the sum can be replaced by an integral over m. The use of Eqs. 19 and 25 shows that

$$dm = \left(\frac{L}{\pi}\right) d\beta_2 = -\left(\frac{L}{\pi}\right) \beta_2^{-1} \, k dk \quad . \quad (31)$$

We take $C=-\pi\rho_w$, as was found for the discrete Pekeris modes in Section II, employ Eqs. 21 and 24, and for the case $0<(d,z)<H$, obtain

$$\varphi_c(r,z) = 2i\left(\frac{\rho_w}{\rho_b}\right)\int_k \frac{\beta_2 \sin(\beta_1 d)\, \sin(\beta_1 z)\, H_o^{(2)}(kr)\, kdk}{\beta_1^2 \cos^2(\beta_1 H) + (\rho_w\beta_2/\rho_b)^2 \sin^2(\beta_1 H)} \quad . \qquad (32)$$

It remains only to find the limits on k or, more precisely, the proper contour. Equation 19 shows that k starts at k_b and decreases along the real axis until k=0. Nothing prevents k^2 from then becoming negative because the separation constant K^2 in Eq. 4 could have been taken with either sign. Hence, integration continues along the imaginary axis of k. The negative axis must be used because $H_o^{(2)}(kr)$--originally chosen in Eq. 9 to ensure outgoing cylindrical waves as $r\to\infty$ --diverges as $+i|k|\to\infty$. The contour of integration in Eq. 32 is, therefore, k_b to 0 to $-i\infty$. Equation 32 is then identical to the branch line integral found by EJP[2] and preferred by Stickler[3] over the corresponding integral of Pekeris.[1]

For the case $d<H$ but $z>H$, $\sin(\beta_1 z)$ of Eq. 32 is replaced by $\mu \sin(\beta_2 z+\nu)$:

$$\varphi_c(r,z>H) = 2i\left(\frac{\rho_w}{\rho_b}\right)\int_k \frac{\sin(\beta_1 d)\, \sin(\beta_2 z+\nu)\, H_o^{(2)}(kr)\, kdk}{\left[\beta_1^2 \cos^2(\beta_1 H) + (\rho_w\beta_2/\rho_b)^2 \sin^2(\beta_1 H)\right]^{1/2}} , \qquad (33)$$

which is identical to the result of EJP. Because there is no longer any distinction between "branch line integral" and "integral over continuous modes," we use the abbreviation BLI for the right-hand sides of Eqs. 32 and 33.

V. Some Properties of the Branch Line Integral

Over the interval $0 \leq k < k_b$, the functions $f(k)$ multiplying $H_o^{(2)}$ in Eqs. 32 and 33 are real and continuous with continuous derivatives. Since kdk becomes $-|k|d|k|$ on $0 \geq k \geq -i\infty$, similar behavior occurs. As $k \to k_b$ on the real axis, β_2 goes to zero and ordinarily $f(k)$ vanishes. However, in the special case that $\beta_1 H$ is an odd multiple of $\pi/2$ at $k=k_b$, $f(k)$ must be tested for a possible singularity. It turns out that $f(k)$ remains finite at k_b (see Appendix A). This case corresponds to having the highest discrete mode occur exactly at cutoff. Both integrands vanish at $k=0$ because $H_o^{(2)}$ has only a logarithmic singularity there.

For any real $k>0$, the asymptotic form of $H_o^{(2)}(kr)$ at large r is a cylindrically spreading and outgoing wave. For $-i|k| \neq 0$, $H_o^{(2)}$ falls off asymptotically as $(|k|r)^{-1/2}\exp(-|k|r)$. To consider the behavior at large z, we must use Eq. 33. For any $\beta_2 \neq 0$, i.e., $k<k_b$, the quantity $\sin(\beta_2 z+\nu)$, regarded as a function of k, oscillates ever more rapidly as z is made larger; therefore the integral approaches zero as $z \to \infty$. Hence, the radiation condition is satisfied for large r and z, which may have seemed doubtful because only standing waves in z, not downward progressing ones, enter Eq. 19.

Eq. 33 ($z>H$) will not be considered further, but Eq. 32 is needed to make a comparison with some of Stickler's results. For sufficiently small $|k|$ on either axis the integrand in Eq. 32 usually approaches $M|k|H_o^{(2)}$, with M being a constant; the first correction terms are in $|k|^3$. (For an exception see Note at the end of Appendix B.) At and near this limit the integral is known in exact form.[11] When k is real and r exceeds zero, the result is

$$\varphi_c = 2i\left(\frac{\rho_w}{\rho_b}\right)\left(\frac{M}{r^2}\right)\int_{kr}^{o} (kr)\, H_o^{(2)}(kr)\, d(kr)$$

$$= -2i\left(\frac{\rho_w}{\rho_b}\right)\left(\frac{M}{r}\right)\left[kH_1^{(2)}(kr) - \left(\frac{2i}{\pi r}\right)\right] \quad . \tag{34}$$

On the negative imaginary axis, with $k=-i|k|$ and $r>0$, we substitute $\zeta=-i|k|$ and find

$$\varphi_c = 2i\left(\frac{\rho_w}{\rho_b}\right)\left(\frac{M}{r}\right)\left[-i|k|H_1^{(2)}(-i|k|r) - \left(\frac{2i}{\pi r}\right)\right] \quad . \tag{35}$$

Therefore the quantities $-(2i/\pi r)$ cancel when Eqs. 34 and 35 are added to integrate "around the corner" near $k=0$. The surviving terms in $H_1^{(2)}$ vanish as $k\to 0$, by mutual cancellation.

If in Eq. 35 the linear approximation $M|k|$ holds for $|k|$ large enough to ensure that $|k|r \gtrsim 2\pi$, then $|H_1^{(2)}(-i|k|r)|$ is not larger than about 6×10^{-4} and decreases rapidly for larger $|k|r$. In contrast, at real $kr\approx 2\pi$, the corresponding term $|H_1^{(2)}(kr)|$ is about 0.3. Apart from its role in canceling the term $(2i/\pi r)$, the integral along the negative imaginary axis is obviously negligible for $|k|r > 2\pi$. The behavior of BLI in Eq. 32 then rests primarily upon the integral from k_b to $k=0$.

It is most unlikely that the integral in Eq. 32 could be evaluated without numerical procedures. Still, additional information about its properties can be gained from analytical approximations. Obvious first comments are that the factor k in $f(k)$ implies only small contributions near $k=0$ and that phase oscillations of the Hankel function will tend to limit the complete result.

Taking the negative of this integral to compensate for inverting the limits to 0 and k_b, we divide the real k axis at points

$k_o=0, k_1,\ldots,k_\ell,\ldots,k_{\ell_b}=k_b$. The intervals need not be equal, but each is to be so small that a sufficient approximation to $f(k)$ is

$$f(k) = m_\ell k + a_\ell \quad , \quad k_{\ell-1} \le k \le k_\ell \quad . \tag{36}$$

Here m_ℓ and a_ℓ, chosen anew for each interval, are always labeled by the higher value of ℓ. This polygonal approximation for $f(k)$ is made continuous across each k_i by requiring that

$$f(k_\ell) = m_\ell k_\ell + a_\ell = m_{\ell+1} k_\ell + a_{\ell+1} \quad . \tag{37}$$

Ignoring the multiplying factor $-2i(\rho_w/\rho_b)$ that precedes the integral, we have

$$\mathcal{I} = \int_o^{k_b} f(k) H_o^{(2)}(kr)dr = \sum_\ell \mathcal{I}_\ell = \sum_\ell \left(\mathcal{I}'_\ell + \mathcal{I}''_\ell \right) , \tag{38}$$

$$\mathcal{I}'_\ell = \left(\frac{m_\ell}{r^2}\right) \int_{k_{\ell-1}r}^{k_\ell r} (kr) H_o^{(2)}(kr) d(kr) \quad , \quad \text{and} \tag{39}$$

$$\mathcal{I}''_\ell = \frac{a_\ell}{r} \int_{k_{\ell-1}r}^{k_\ell r} H_o^{(2)}(kr) d(kr) \quad . \tag{40}$$

$\mathcal{I}'_\ell$ has the same form as the integral in Eq. 34; the whole term is, therefore,

$$\left[k_\ell H_1^{(2)}(k_\ell r) - k_{\ell-1} H_1^{(2)}(k_{\ell-1} r) \right] \quad . \tag{41}$$

There is an exception when $k_{\ell-1}=k_o=0$, for then the last term in Eq. 41 is replaced by $-(2i/\pi r)$ as in Eq. 35. However, this quantity is canceled by a like contribution from the integral over imaginary k (Eqs. 34, 35) and will be ignored. Handling $\sum \mathcal{I}_{,\ell}$ and combining it with $\sum \mathcal{I}_{\ell}$ is more complicated; we relegate the details to Appendix B.

The outcome (Eq. B13) is

$$\varphi_c \approx 2i^{3/2}\left(\frac{\rho_w}{\rho_b}\right)\left(\frac{2}{\pi}\right)^{1/2} r^{-5/2} \times \left[m_{\ell_b} k_b^{-1/2}\, e^{-ik_b r} - \sum_{\ell=1}^{\ell_b-1} (m_{\ell+1}-m_\ell) k_\ell^{-1/2}\, e^{-ik_\ell r}\right]. \tag{42}$$

Evidently the main contributions of BLI to the mode sum will stem from f(k) having a slope of large magnitude near $k=k_b$ and/or from parts of the finite sum being large. The term $m_{\ell+1}-m_\ell$ for the polygonal approximation to f(k) is roughly proportional to d^2f/dk^2. Thus, large contributions to the mode integral come from intervals Δk in which the slope of f is changing rapidly. For example, suppose that in some part of $0<k<k_b$ the function f(k) has a high narrow "spike" which is almost a triangle. The polygonal approximation might then employ only two intervals: ℓ-1 to ℓ and ℓ to ℓ+1; m_ℓ would be large and positive and $m_{\ell+1}$, large and negative. Over these two intervals, $k_\ell^{-1/2}$ would change only slightly. If, in addition, r were not too large so that $\exp(-ik_\ell r)$ did not change greatly, this contribution to BLI would be a virtual mode with an eigenvalue k_ℓ^2. As r increases, however, both the factor $r^{-5/2}$ and the phase oscillating exponential term would make the virtual mode become rapidly less important.

VI. Locating Resonances and Virtual Modes

As we have said before, eventually BLI must be evaluated numerically. However, it is simple to name approximate locations of the resonances described in Section V. From Eqs. 14, 19, and 32, we have

$$f(k) = \frac{k\beta_2 \sin(\beta_1 d) \sin(\beta_1 z)}{\beta_1^2 \cos^2(\beta_1 H) + (\rho_w \beta_2/\rho_b)^2 \sin^2(\beta_1 H)} \quad , \text{ and} \qquad (43)$$

$$\beta_1 = \left(k_w^2 - k^2\right)^{1/2} \quad ; \quad \beta_2 = \left(k_b^2 - k^2\right)^{1/2} \quad . \qquad (44)$$

Only real k, $0 \leq k \leq k_b$, is considered. The constant $(\rho_w/\rho_b)^2$ in the denominator would usually be some 0.25 to 0.5. Because Eq. 32 holds only for $(d,z) < H$, $\beta_1 d$ and $\beta_1 z$ in the numerator will be smaller than $\beta_1 H$. The product of the two sine functions will oscillate (unless d=z). For k far enough from zero, the product can change sign; on the average, it does little else. For sufficiently small k, β_1 and β_2 are approximately k_w and k_b, respectively, and the denominator remains nearly constant. The magnitude of the numerator initially rises roughly in proportion to k; for larger k, it may develop some oscillations about this linear rise.

As k increases enough so that β_1 and β_2 are no longer nearly constant, the denominator begins to govern f(k). For sufficiently large $k_b H$, the angle $\beta_1 H$ goes through whole cycles in which the cosine (sine) term vanishes when $\beta_1 H$ is an odd (even) multiple of $\pi/2$. For some range of intermediate k, nothing exciting happens because the oscillations of $\cos^2$ and $\sin^2$ roughly balance each other. As k comes close enough to k_b, however, β_1 and especially β_2 change more rapidly with k. β_1 can never be less than $(k_w^2 - k_b^2)^{1/2} > 0$, but β_2 approaches zero. In this range of larger k, when $\beta_1 H \approx (2n+1)(\pi/2)$, the cosine term becomes very small. The sine term itself is nearly unity but it is multiplied by a term smaller than β_2^2. Hence, the whole denominator becomes small and $|f(k)|$ becomes large rather abruptly. As k and $\beta_1 H$ pass through this critical region, $|f(k)|$ decreases again, about equally abruptly.

It follows that the locations of large resonances in f(k), with consequent virtual modes, are determined by two simultaneous conditions: (1) k being not too far from the branch point $k=k_b$ and

(2) $\beta_1 H \approx (2n+1)\pi/2$. Moreover, the resonance will be stronger and narrower the nearer condition 2 gets to $k=k_b$. Conditions 1 and 2 are necessary but not sufficient for appearance of a resonance because the magnitude of the numerator might be very small where resonance would otherwise have been predicted. We note that substantial resonances cannot occur on the imaginary axis of k because $\beta_2 \geq k_b$ remains large everywhere. It is interesting to observe that conditions 1 and 2 are also the requirements for explaining the bottomborne first arrival.[12]

Even for fairly low frequency in shallow water, a few resonances are possible. As frequency and water depth increase, i.e., as H/λ increases, the number of potential resonances rises. An approximate upper bound is the number of integers in the range $k_w H/\pi$ to $(k_w^2 - k_b^2)^{1/2} H/\pi$.

VII. Application to Stickler's Figure 11

Stickler has published numerical calculations of transmission loss versus range for different sets of assumed conditions.[3] His Fig. 8 approximates a Pekeris case in shallow water, with H=150 ft, d=20 ft, and z=40 ft. There is a slight decrease of c(z) with depth in the water layer but there is a constant c_b and a density ratio of 1.4. At a frequency of 100 Hz, there is one discrete mode. Plotted against range r from less than 1000 ft out to 21,000 ft, Stickler's Fig. 11 shows transmission loss at 100 Hz. The figure gives separately the contribution of the one discrete mode and the contribution of the discrete mode plus BLI. Moreover, as a matter of particular interest for the present analysis, Bartberger had contributed 20 points spaced along the discrete-plus-continuous curve and computed by his method of improper modes.[4,5] His agreement with Stickler's plotted curve is everywhere good.

Since postulate 2 (Section I) rules out improper modes, we seek another explanation of this agreement in terms of Sections V and VI. The first step, approximating Stickler's Fig. 8 by a Pekeris problem, required the estimating of a constant average c_w in the water layer. Otherwise, his data were retained. At 100 Hz, the chosen values were k_w=0.125916 and k_b=0.124223. The eigenvalue of the one discrete mode, found numerically from Eq. 16, corresponds to k_1=0.125068.

Next, f(k)--Eq. 43--was calculated numerically at some 50 values of k, widely spaced where f varied slowly but more closely spaced in the two dominant resonances. Figure 1 sketches f(k), from k=0.04 to k_b. For k<0.04, f(k) merely falls slowly and monotonically. Five points at which $\cos(\beta_1 H)$ vanishes were found. In Fig. 1 they are marked with circles enclosing the pertinent values of 2n+1.

Obviously only the last two resonances, appearing toward $k=k_b$, are significant. These parts of the curve were calculated at smaller intervals and the two maxima were located with moderate care (at k_I=0.11482 and k_{II}=0.121934). Thereafter f(k) was regarded as basically a function $f_o(k)$ to which the resonances were added. f_o coincides with f(k) for $k \lesssim 0.105$, but then it is considered to vary so smoothly before vanishing at k_b that its contribution to φ_c (Eq. 42) is negligible. Each resonance was numerically fitted by a gaussian,

$$\left(\frac{2\rho_w}{\rho_b}\right)\left[f(k) - \langle f_o \rangle\right] = a \exp(-b\kappa^2) \quad ; \qquad (45)$$

κ is $k-k_{I,II}$, as pertinent, and $\langle f_o \rangle$ is an average value of $f_o(k)$ over the base of each spike. The constants were a_I=3.551, b_I=1.632x10^5, a_{II}=8.040, and b_{II}=6.56x10^5. These gaussians fitted the resonances fairly well except that they somewhat overemphasized the discreteness of the "spikes" (see Fig. 1) by lowering and sharpening the intermediate minimum.[13]

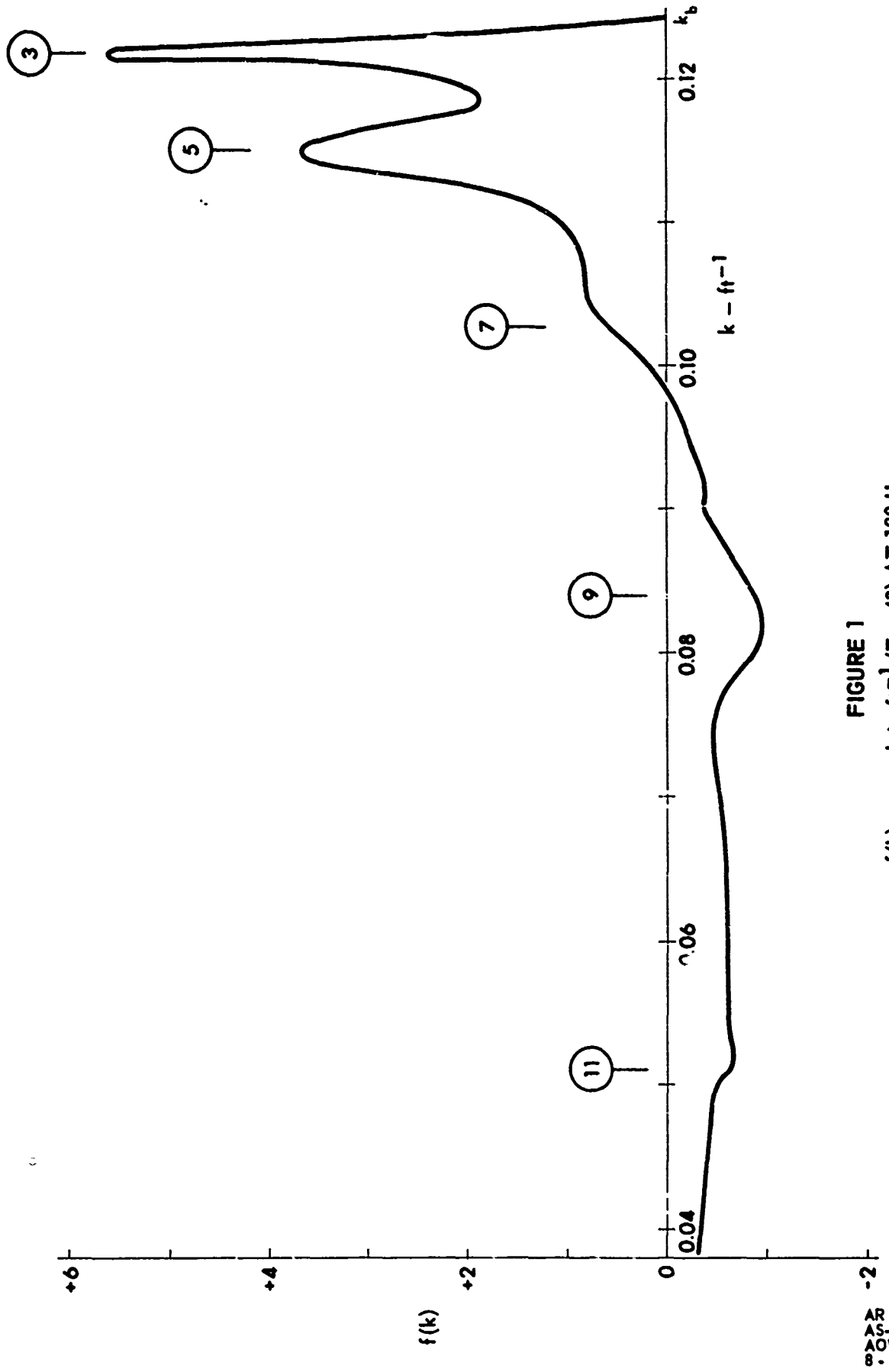

FIGURE 1

f(k) versus k in ft^{-1} (Eq. 43) AT 100 Hz
CIRCLED NUMBERS: $\beta_n + 1$ IN $\beta_n H = (2n+1)\pi/2$

ARL - UT
AS-76-1005
AOW - RFO
8 - 30 - 76

In this range of k, even for r being much smaller than any values shown in Stickler's Fig. 11, $H_o^{(2)}(kr)$ is given with great precision by its asymptotic form, Eq. B9, with $x=(k_{I,II}+\kappa)r$. Moreover, $(\kappa r)^{1/2}$ is very well approximated by $(k_{I,II}r)^{1/2}$ because the resonances are narrow. Then the contribution Δ_I to φ_c from resonance I is

$$\Delta_I \approx \left(\frac{2}{i\pi k_I}\right)^{1/2} r^{-1/2}\, e^{-ik_I r}\, a_I \times \int_{-\infty}^{\infty} \exp(-b_I\kappa^2)\, e^{-i\kappa r}\, d\kappa \quad . \quad (46)$$

The same expression, with subscripts II, holds for the other resonance. The integral is a standard form and the numerical results are (with r in feet)

$$\Delta_I \approx 0.03669\, i^{-1/2}\, r^{-1/2} \exp(-1.532 \times 10^{-6} r^2) \exp(-0.11482ir) \quad ; \quad (47)$$

$$\Delta_{II} \approx 0.04020\, i^{-1/2}\, r^{-1/2} \exp(-3.811 \times 10^{-7} r^2) \exp(-0.121934ir) \quad . \quad (48)$$

The contribution Δ_M of the one discrete mode is

$$\Delta M \approx 0.01495 i^{-1/2}\, r^{-1/2} \exp(-0.125068ir) \quad . \quad (49)$$

Equations 47 through 49 show that the virtual modes attributable to resonances I and II behave like discrete modes except for the real exponentials in r^2. The coefficient of r^2 is inversely proportional to the constant b in Eq. 45. Therefore, regardless of a resonance's height, the virtual mode derived from a narrower resonance falls off more slowly with increasing range. A virtual mode must decrease more rapidly with range than does a discrete mode. The reason is seen in the integral of Eq. 46. The subset of continuous modes that make up a resonance embraces a small spread of k and therefore of κ. Regardless of range, this spread is governed by the gaussian in Eqs. 45 and 46. For sufficiently small r, $\exp(i\kappa r)$ in Eq. 46 is nearly unity; the modes in this subset are substantially in phase. As r increases,

however, $\exp(-i\kappa r)$ oscillates in phase over the practical spread of κ, and the continuous modes interfere even more destructively. In the limit when a resonance is well approximated by a delta function in κ, the consequent virtual mode falls off only as $r^{-1/2}$, just as a discrete mode does. (With their different fit[13] to a resonance, Tindle and Guthrie[7] found an excess falloff in the form of a decaying exponential in r, not r^2; however, the physical cause is the same.)

A few numerical trials showed that for $r \leq 1000$ ft, all three modes interact appreciably as their phases change with r. Before r=2000 ft is reached, only II and M interact significantly; I has fallen too much in amplitude. Eventually, mode II fades out also, and a plot of transmission loss becomes essentially smooth and monotonic.

Numerical values of $|\Delta|^2$ were calculated at various values of r by using the mode sum

$$\Delta = \Delta_M \left[1 + \left(\frac{\Delta_I}{\Delta_M} \right) + \left(\frac{\Delta_{II}}{\Delta_M} \right) \right] \quad . \tag{50}$$

Three extrema in the interval $1000 \lesssim r \lesssim 3000$ ft were located near the corresponding ranges in Fig. 11 of Ref. 3. Long before r=3000 ft is reached, Δ_I has become negligible $|\Delta_{II}|$ is so small that the factor r^{-1} from $|\Delta_M|^2$ hides any extremum. However, a weak maximum of $r|\Delta|^2$ lay near r=3000 ft. Two still weaker extrema were found at greater ranges by the differentiation of an analytical approximation to $r|\Delta|^2$.

These six ranges are listed in line (W) of Table I; line (S) gives Stickler's corresponding ranges.[14]

TABLE I

COMPARISON OF RANGES r (IN feet) AT WHICH EXTREMA OF THE MODE SUM OCCUR

Extremum	Min.	Max.	Min.	Max.	Min.	Max.
(W) r	1170	1700	2950	3770	4740	5710
(S) r	1120	1740	3000	3820	5420	5660
Discrepancy	4.5%	2%	2%	1%	14%	1%

Agreement for the first four entries is good. The average magnitude of fractional discrepancy, 2.4%, is quite acceptable in view of our numerical approximations and the uncertainty in reading ranges from Stickler's graph. Our last two extrema are so weak that even minor changes in the underlying parameters could alter their locations considerably. Hence, neither the good nor the bad case is particularly significant. The unweighted average value for magnitudes of fractional discrepancies for all six cases is only 4%. The ranges in line (W) are fixed primarily by the values of k_I, k_{II}, and k_M, but the real exponentials in r^2 (Eqs. 47 and 48) have an appreciable influence.

A comparison of our results with Stickler's appears in Fig. 2 where the calculated transmisssion loss TL in decibels,

$$TL = 10 \log_{10}(|\Delta|^2) \quad , \tag{51}$$

is plotted versus range r in feet. The dotted line corresponds to const./r, i.e., to "ARL Discrete" of Fig. 11, Ref. 3, or simply to $|\Delta_M|^2$ for the discrete mode. This curve was used to make the vertical scaling agree with Stickler's graph. The broken dashed line is "ARL Discrete Plus Continuous" of Ref. 3. The full line illustrates our results; vertical arrows mark the last two extrema of Table I. Beyond r=4000 ft, the full and dotted lines are essentially indistinguishable, as are the dashed and dotted lines for r≳7500 ft, because BLI has

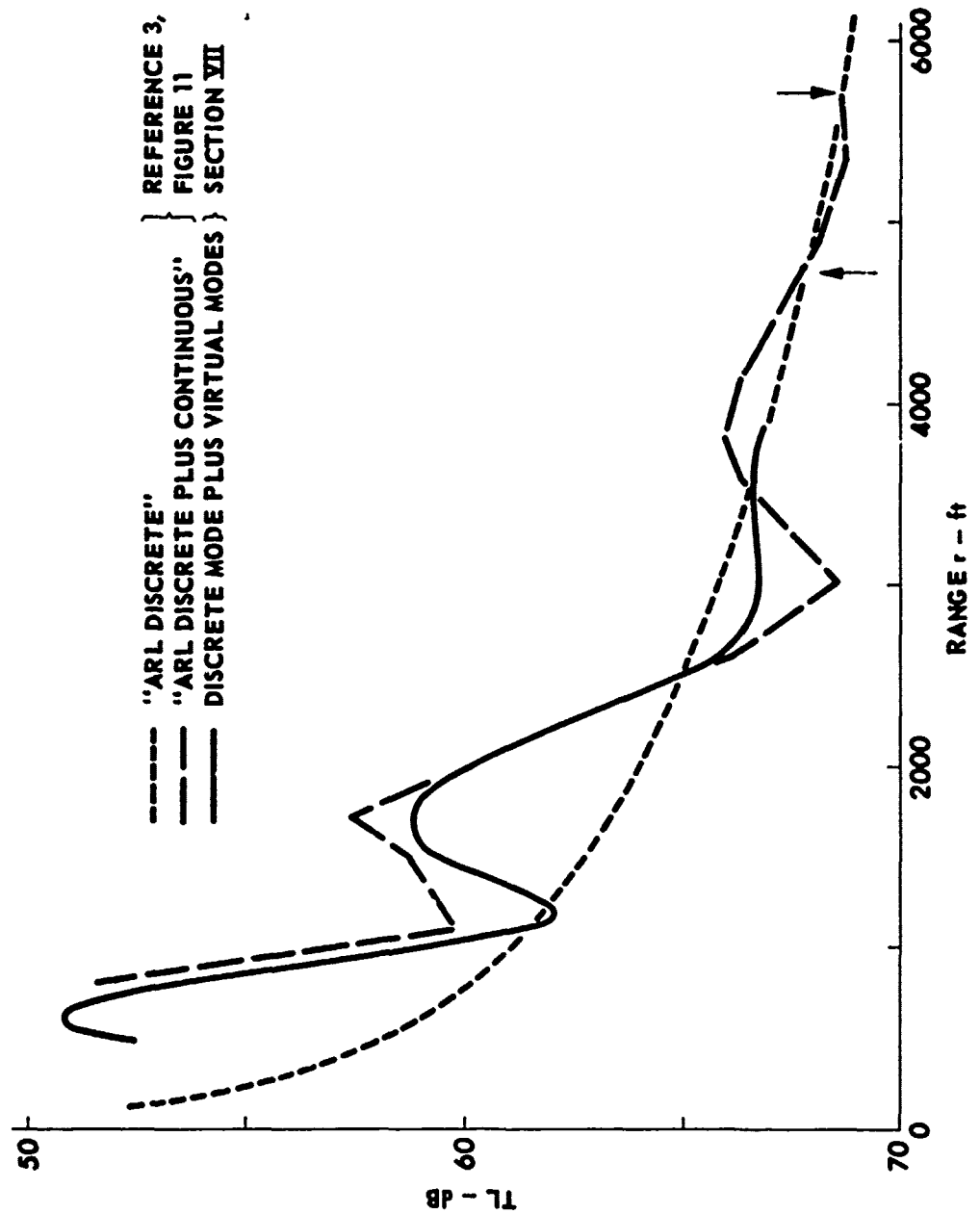

FIGURE 2
TRANSMISSION LOSS (TL) versus RANGE r

ARL - UT
AS-76-1006
AOW - RFO
8 - 30 - 76

become negligible. Between r=2000 and r=2500 ft, the full and the dashed curves practically coincide.

The full line represents chiefly the sum, with interaction, of modes M and II. In the range $500 \lesssim r \lesssim 1500$ ft, however, the weaker virtual mode I contributes appreciably. Omitting it would have markedly weakened the agreement with Stickler's result. For $r \gtrsim 2500$ ft, mode I is negligible and mode II has decayed with range much too fast to yield anything close to the dashed line. Replacing Eq. 45 by a better analytical fit[13] with its slower decay in range might improve agreement beyond 2500 ft.

The degree of success out to r≈2500 ft, before the excessive decay rate of mode I becomes important, is gratifying when it is remembered that we have used only a Pekeris approximation to Stickler's Fig. 8. In particular, the arguments in Sections V and VI that only the strong resonances need be included in evaluating BLI are supported by Fig. 2. Although no direct analytical connection has been shown with Bartberger's improper modes, we have at least found that resonances in BLI can produce similar results. A little more information emerges in Section VIII.

VIII. Application to Stickler's Figure 10

Figures 10 and 11 of Ref. 3 differ only in respect to frequency--50 Hz for Fig. 10 and 100 Hz for Fig. 11. Stickler found that a single discrete mode, near cutoff, still exists at 50 Hz. The two plots in Fig. 10--"ARL Discrete" (AD) and "ARL Discrete Plus Continuous" (ADC) are quite unlike their counterparts in Fig. 11. First, out to the extreme range of calculations (r≈90,000 ft) ADC of Fig. 10 lies several decibels above AD instead of converging to it for $r \gtrsim 7000$ ft. Second, ADC shows no indication of mode interaction. Third, Bartberger's calculated points now fall on AD, not ADC.

Numerical trials suggested that ADC could be fitted by the sum of two terms, one varying as $r^{-1/2}$ (presumably the discrete mode) and the other (of much larger amplitude) varying approximately as r^{-1} (presumably from BLI). When a discrete mode is quite near cutoff, a BLI contribution in r^{-1} is to be expected.[12,15,16]

To make quantitative comparisons, we proceed as before by fitting a Pekeris approximation to Stickler's Fig. 8. A trial value of c_w, 4985 ft/sec, was chosen near the average of the varying c_w in Fig. 8, and the eigenvalue k_1^2 of the discrete mode was calculated from Eq. 16. The modes being near cutoff implies that its properties are highly sensitive to the value of k_1^2. A better eigenvalue was sought by using Stickler's actual $c_w(z)$ as the basis for a first order perturbation correction.[17] The result, k_1=0.0621123, differed only a little from the first try. A new constant value, c_w=4985.73 ft/sec, was found to agree with the revised k_1. Next, the normalization constant N_1 was calculated from Eq. 18. Near cutoff, the eigenfunction retains appreciable amplitude deep into the bottom. Consequently, N_1 is quite small; the discrete mode amplitude is only about 5% of that in Eq. 49.

Numerical calculations of f(k) revealed a pronounced spike with a peak very near $k=k_b$. (This spike, a "pseudoresonance," is less than half of a true resonance. It rises smoothly as $k\to k_b$ and then is abruptly reduced to zero by the factor β_2 in the numerator of Eq. 43. The actual resonance condition on $\beta_1 H$ could be met only for $k>k_1$.) No significantly strong resonance was found at smaller k. Across the spike, k varies only slightly, whereas β_2 is much smaller and varies rapidly. Hence, it seemed best to change variable from k to $\kappa=\beta_2$, as in Appendix A and Ref. 7, replacing f(k)dk in BLI by $g(\kappa)d\kappa$. Expanding f(k) in powers of κ showed that over the width of the spike, g is well represented by

$$g(\kappa) = \frac{a\kappa^2}{(1+b\kappa^2)} \quad . \tag{52}$$

The constants a and b can be found analytically, but as a measure of correction for higher terms omitted from Eq. 52 they were instead determined empirically to fit numerical values of g. To obtain known functions from integration of g over the spike, Eq. 52 was curve fitted to another form,

$$g(\kappa) = \left(\frac{a}{b}\right)[1 - \exp(-A\kappa)] \quad . \tag{53}$$

Agreement with Eq. 52 was good (within an average 2% wherever g was of substantial size). The Hankel function in BLI was again replaced by its asymptotic form for large kr (Eq. B9), and k was expressed (to better than a part in 10^5 over pertinent κ's) by

$$k = k_b - \frac{\kappa^2}{2k_b} \quad . \tag{54}$$

Equation 32, confined to the spike, becomes

$$\varphi_c = -2iC'\left(\frac{\rho_w}{\rho_b}\right)\left(\frac{2i}{\pi k_b r}\right)^{1/2} \exp(-ik_b r)$$

$$\times \left\{ \int_0^\infty \exp\left(\frac{i\kappa^2 r}{2k_b}\right) dk - \int_0^\infty \exp\left[\left(\frac{i\kappa^2 r}{2k_b}\right) - A\kappa\right] d\kappa \right\} \quad . \tag{55}$$

Here C' is a combination of constants already mentioned. The upper limit of κ is safely extended to infinity because the spike is narrow. The expressions in { } can be converted to standard forms in terms of Fresnel integrals.[18] The discrepancy $\Delta g(\kappa)$ between Eq. 52 and 53 is small in amplitude and is very narrow. A rough calculation, based upon a

triangular fit to Δg, showed that its contribution to φ_c varies nearly as $r^{-1/2}$ and in amplitude is less than 1% of the discrete mode.

The total contribution Δ to φ is

$$\Delta = 7.0 \times 10^{-4}(ir)^{-1/2} \exp(-ik_1 r)$$

$$+ 0.227\, r^{-1} \exp(-ik_b r)[1 + (1+i)(f+ig)] \quad . \qquad (56)$$

The first term comes from the discrete mode and the second, from the pseudoresonance; f and g, functions of $(350/r^{1/2})$, are defined and tabulated in Ref. 18. The second term in Eq. 55 is larger than the extreme asymptotic result found through a different method by Brekhovskikh.[15] k_1 and k_b in Eq. 55 are so nearly equal that even for r=90,000 ft the two exponentials differ negligibly in phase--another reason for the absence of appreciable mode interaction in Stickler's Fig. 10. The magnitude of Eq. 56, converted to decibels, is our approximation to ADC in Fig. 10 of Ref. 3. The first term in Eq. 56, similarly converted, corresponds to AD.

When (as in Section VII) it is assumed that our AD and Stickler's are identical, our calculated ADC differs from his by no more than 0.1 to 0.2 dB, which is within the uncertainty of reading his graph. It appears that Fig. 10 is adequately explained as the combination of a single discrete mode and a virtual mode from a pseudoresonance induced by the discrete mode's being very near cutoff.

The assumption that our AD and Stickler's can be equated may seem gratuitous because we have dealt only with a Pekeris approximation to Stickler's Fig. 8. With respect to our Section VII and Fig. 2, there could well be doubt. At short ranges the one discrete mode and the two virtual ones are of comparable amplitudes, and appreciable

changes in any one amplitude would not greatly alter Fig. 2. The good results in this present section, however, seem to validate the assumption. Suppose, for example, that our Pekeris approximation drove the discrete mode too close to cutoff. Then $\beta_1 H$ is pushed downward too close to the value $\pi/2$. Our pseudoresonance and the virtual mode are made too strong. Simultaneously, the discrete mode is made too weak because the term $|\tan(\beta_1 H)|$ in Eq. 18, which strongly dominates the value of N_1, becomes too large and makes N_1 too small. Therefore, our calculated differences between AD and ADC would have been decidedly larger than Stickler's differences. A similar argument would hold, of course, if our discrete mode had been too far from cutoff; our AD and ADC would have been too close together.

Two speculative comments might be added. The first concerns the abrupt shift of Bartberger's calculated points from lying on AD in Fig. 10 of Ref. 3 to lying on ADC in Fig. 11. It would appear that for some reason not yet clear, the method of improper modes can duplicate the effects of true resonances within BLI and the consequent virtual modes, but that it does not detect a pseudoresonance caused by a discrete mode very near cutoff. (The method would, of course, recognize and use that discrete mode as well as any others that might be present.)

The second comment concerns Kutschale's computed points, shown in Fig. 10 of Ref. 3. These points might be interpreted as showing mode interaction between the discrete mode and BLI--a small effect in amplitude, but much larger than any found by Stickler and by us. One implication would then be that Kutschale's discrete mode and BLI are much nearer in amplitude than we have found. A more definitive test is afforded by the corresponding interaction distance Δr (defined by $\Delta r = 2\pi/\Delta k$, where in our calculation Δk is $k_1 - k_b$). Kutschale's Δr can be roughly estimated as 45,000 to 60,000 ft; in sharp contrast, our Δr would be about 8×10^6 ft. This seeming interaction may be only an accidental result, but in any event, it shows that different computer methods can lead to noticeably different results.

IX. Summary

Under the restrictions of constant water depth, only vertical variations in parameters, no absorption, and a bottom that can be treated as a fluid half-space, Sections I through IV give the normal mode method for propagation of underwater sound. The language of eigenfunctions and eigenvalues is used, with no recourse to integration in the complex plane. Only an omnidirectional point source, cw at a single frequency, is used. Except perhaps for the two postulates in Section I, nothing new is presented; the goal was a compendium. For the Pekeris problem, it was demonstrated that the integral over the "continuous" modes is identical to the branch line integral (BLI) found by Ewing, Jardetzky and Press[2] through use of integration in the complex plane. (Tindle and Guthrie have independently and simultaneously derived the same result.)[7] Since the BLI of Ref. 2 differs from that of Pekeris,[1] the outcome is of interest.

Sections V and VI, supplemented by Appendices A and B, discuss properties of the BLI, i.e., the integral over continuous modes, for the Pekeris problem. It is proved analytically that, piecewise, BLI contributes practically negligibly to the sound field except where the integrand displays narrow "spikes" or <u>resonances</u> (see Fig. 1). The conditions for such resonances to exist with the consequent production of <u>virtual modes</u>[6,7] are demonstrated. (Again, Ref. 7 covers much of the same ground although with a different but equivalent integral and with less analytical proof.)

Finally, in Sections VII and VIII the preceding methods are used to afford comparisons with some computer calculations by Stickler[3] (specifically, his Figs. 8, 10, and 11). For this purpose, his assumed model was approximated by a Pekeris problem. Reasonably good agreement is shown with his Fig. 11 (our Table I and Fig. 2) and excellent agreement, with his Fig. 10. Advantages of the semianalytic method used here are that (1) a partial separation of range variation is

effected and (2) fairly simple explanations are afforded of such considerable differences as those between Stickler's Fig. 10 and Fig. 11.

An empirical conclusion about Bartberger's method of improper modes[4,5] is presented; it is based only upon specific results found here. That method seems able to duplicate the effect (virtual modes) of true resonances in BLI but not to handle the behavior of BLI when a discrete mode is near cutoff.

ACKNOWLEDGEMENTS

This work was sponsored by Naval Electronic Systems Command, Code 320.

It is a pleasure to acknowledge helpful correspondence with C. L. Bartberger, R. N. Denham, D. C. Stickler, ar ' . T. Tindle.

APPENDIX A

QUESTION OF A SINGULARITY IN EQ. 32

At the beginning of Section V it was suggested that the integrands of Eqs. 32 and 33 might have singularities at $k=k_b$, where β_2 vanishes, provided also that $\beta_1 H=(n+1/2)\pi$ there. We now show that no singularity exists. Using Eqs. 14 and 19 for β_1 and β_2 (with k_n^2 replaced by k^2) and abbreviating $k_w^2-k_b^2$ as K^2 and β_2 as κ, we have

$$\beta_1 = + (K^2+\kappa^2)^{1/2} \quad . \tag{A1}$$

In Eq. 32 we multiply numerator and denominator by $\delta^2=(\rho_b/\rho_w)^2$ and at first consider only the resulting denominator $D(\kappa)$, assuming, of course, that neither $\sin(\beta_1 d)$ nor $\sin(\beta_1 z)$ vanishes at $k=k_b$:

$$D(\kappa) = \delta^2\beta_1^2 - (\delta^2\beta_1^2-\kappa^2)\sin^2(\beta_1 H)$$

$$= \delta^2\beta_1^2 - (\delta^2\beta_1^2-\kappa^2)\cos^2\theta \quad ; \tag{A2}$$

$$\theta = (n+1/2)\pi - \beta_1 H \quad . \tag{A3}$$

These equations are exact. We now assume that k is so near k_b, where both κ and $\cos(\beta_1 H)$ vanish, that $\kappa^4 \ll K^4$ and $\theta^4 \ll (\pi/2)^4$. The consequences are that

$$\cos^2\theta = 1 - \theta^2 + \ldots \quad ; \quad \beta_1 H = KH + \left(\frac{H}{2K}\right)\kappa^2 + \ldots \quad . \tag{A4}$$

The first omitted terms are in θ^4 and κ^4. Since $\beta_1 H \to (n+1/2)\pi$ as $\kappa \to 0$, evidently KH equals $(n+1/2)\pi$. Equations A3 and A4 yield

$$\theta = -\left(\frac{H}{2K}\right)\kappa^2 + O(\kappa^4) \quad . \tag{A5}$$

Finally, Eqs. A2, A4, and A5 show that

$$D(\kappa) = \kappa^2[1 + O(\kappa^2)] \quad . \tag{A6}$$

Returning to Eq. 32, we see in the numerator a factor $\beta_2=\kappa$ and the quantity kdk. Since $\beta_2^2=\kappa^2$ is $k_b^2-k^2$, it follows that $kdk=-\kappa d\kappa$. Accordingly, κ^2 cancels in numerator and denominator. The integrand of Eq. 32 does not vanish at $k=k_b$, but remains finite.

Equation 33, which we have not used, behaves itself similarly. In comparison to Eq. 32, it lacks the factor β_2 in the numerator, but its denominator becomes $D^{1/2}\propto\kappa$, instead of $D\propto\kappa^2$.

APPENDIX B

EVALUATION OF $\sum \ell_i''$ IN EQS. 38 THROUGH 40

The pertinent integral for $\mathcal{I}_\ell''$ is known[B1]:

$$\mathcal{I}_\ell'' = \left(\frac{a_\ell}{r}\right)\left\{ x\, H_o^{(2)}(x) + \frac{\pi x}{2}\left[\mathbf{H}_o(x)H_1^{(2)}(x) - \mathbf{H}_1(x)H_o^{(2)}(x)\right]\right\} \Bigg|_{x=k_{\ell-1}r}^{k_\ell r} \tag{B1}$$

The $\mathbf{H}$'s are Struve functions.[B2] Continuing with the abbreviations $x=kr$, $x_\ell=k_\ell r$, and $x_{\ell-1}=k_{\ell-1}r$, we write

$$\mathbf{H}_o(x) = Y_o(x) + P(x) \quad ; \quad \mathbf{H}_1 = Y_1(x) + Q(x) \quad . \tag{B2}$$

Equations B2 are unexceptionable provided that P and Q are defined properly; we choose this form with an eye on later use of asymptotic expressions.[B3] Substituting Eqs. B2 in Eq. B1 and using the definitions of Hankel functions,

$$H_{o,1}^{(2)}(x) = J_{o,1}(x) - iY_{o,1}(x) \quad , \tag{B3}$$

we obtain

$$\mathcal{I}_\ell'' = \left(\frac{a_\ell x}{r}\right)\left\{ H_o^{(2)}(x) - \frac{\pi}{2}\left[J_o(x)Y_1(x) - J_1(x)Y_o(x)\right] + \left(\frac{\pi}{2}\right)P(x)H_1^{(2)}(x) - \left(\frac{\pi}{2}\right)Q(x)H_o^{(2)}(x)\right\} \Bigg|_{x_{\ell-1}}^{x_\ell} \quad . \tag{B4}$$

The [ ] in Eq. B4 has the value[B4] $(2/\pi x)$. Let us express P and Q in terms of $p(x)$ and $q(x)$:

$$P(x) = \left(\frac{2}{\pi x}\right)[1 + p(x)] \quad ; \quad Q(x) = \left(\frac{2}{\pi}\right)[1 + q(x)] \quad . \qquad (B5)$$

Equation B4 reduces to the form

$$\mathcal{I}_\ell'' = \left(\frac{a_\ell}{r}\right)[1 + H_1^{(2)}(x) + p(x)H_1^{(2)}(x) - xq(x)H_o^{(2)}(x)] \Big|_{x_{\ell-1}}^{x_\ell} \quad . \qquad (B6)$$

When $\mathcal{I}_\ell''$ is evaluated at its limits and the result is added to $\mathcal{I}_\ell'$ (Eq. 41), and after Eq. 37 is used, we find for $\mathcal{I}_\ell = \mathcal{I}_\ell' + \mathcal{I}_\ell''$:

$$\mathcal{I}_\ell = r^{-1}[f(k_\ell)H_1^{(2)}(k_\ell r) - f(k_{\ell-1})H_1^{(2)}(k_{\ell-1}r)]$$

$$+\left\{\left(\frac{a_\ell}{r}\right)[p(k_\ell r)H_1^{(2)}(k_\ell r) - p(k_{\ell-1}r)H_1^{(2)}(k_{\ell-1}r)]\right\} \qquad (B7)$$

$$-\left\{\left(\frac{a_\ell}{r}\right)[k_\ell r\, q(k_\ell r)H_o^{(2)}(k_\ell r) - k_{\ell-1}r\, q(k_{\ell-1}r)H_o^{(2)}(k_{\ell-1}r)\right\} \quad .$$

The next step is to sum $\mathcal{I}_\ell$ from ℓ-1=0 (at k=0) to ℓ_b, corresponding to $k_{\ell_b}=k_b$. The first bracket in Eq. B7 leads to a telescoping sum that reduces to its first term (k=0) and to its last ($k=k_b$). We recall from the comment after Eq. 41 that a term $-2i/\pi r$ is to be ignored. But f(0) vanishes, and so does $f(k_b)$ except in the unlikely event discussed at the start of Section V. We disregard this special case (see Appendix A). Accordingly, the first bracket in Eq. B7 sums to zero.

The remaining two terms of Eq. B7 in { } are nominally to be summed starting with ℓ-1=0, i.e., k=0 and ℓ=1. However, in the first interval k_o to k_1 the function f(k) vanishes at k=0; therefore a_1 is identically zero. The sum is, then, from ℓ=2 to ℓ_b. It appears safe to replace p(x) and q(x) by their first asymptotic terms[B3] (respectively

$-1/x^2$ and $+1/x^2$), which fall off as $1/r^2$. The next asymptotic terms go much faster, as $1/r^4$. In contrast, each discrete mode falls off asymptotically only as $r^{-1/2}$. The summand in Eq. B7 is now

$$\mathcal{I}_\ell = -\left(\frac{a_\ell}{r}\right)\Big\{(k_\ell r)^{-2}H_1^{(2)}(k_\ell r) + (k_\ell r)^{-1}H_o^{(2)}(k_\ell r)$$

$$+\left(\frac{a_\ell}{r}\right)(k_{\ell-1}r)^{-2}H_1^{(2)}(k_{\ell-1}r) + (k_{\ell-1}r)^{-1}H_o^{(2)}(k_{\ell-1}r)\Big\} \quad . \tag{B8}$$

At this point we replace the Hankel functions $H_o^{(2)}$ by the first terms of their asymptotic expressions:

$$H_o^{(2)}(x) \sim \left(\frac{2}{\pi x}\right)^{1/2} e^{i\pi/4}\, e^{-ix} \quad . \tag{B9}$$

For the same arguments x, $H_1^{(2)}$ and $H_o^{(2)}$ have equal magnitudes, but the terms in $H_1^{(2)}$ are multiplied by $1/r^2$, not $1/r$ as for those in $H_o^{(2)}$. Hence, we retain only the latter terms. (Discarding $H_1^{(2)}$ is not essential. It could be retained and handled as we proceed below. In that event, however, the first term omitted from Eq. B9 should also be used.) Equation B8 becomes

$$\mathcal{I}_\ell = -\left[\left(\frac{2}{\pi}\right)^{1/2} e^{i\pi/4}\, r^{-5/2}\right] a_\ell\left(k_\ell^{-3/2}\, e^{-ik_\ell r} - k_{\ell-1}^{-3/2}\, e^{-ik_{\ell-1}r}\right) \quad . \tag{B10}$$

When the portion of Eq. B10 that depends upon ℓ is summed, it is found to telescope in part, leaving

$$\mathcal{I} = [\;]\left\{-a_{\ell_b} k_{\ell_b}^{-3/2}\, e^{-ik_{\ell_b} r} + \sum_1^{\ell_b-1}(a_{\ell+1}-a_\ell)k_\ell^{-3/2}\, e^{-ik_\ell r}\right\} \quad . \tag{B11}$$

From Eq. 38 it is evident that

$$a_{\ell+1} - a_\ell = -k_\ell(m_{\ell+1}-m_\ell) \quad , \quad 1 \le \ell \le \ell_b \quad . \tag{B12}$$

From the same equation, it follows that $f(k_\ell)=m_\ell k_\ell+a_\ell$ at $\ell=\ell_b$, but there, ordinarily, f vanishes. Hence we can replace a_{ℓ_b} by $-m_{\ell_b}k_{\ell_b}$.

Restoring the factor $-2i(\rho_w/\rho_b)$ omitted after Eq. 37 and recalling that we have calculated the negative of BLI, we obtain finally

$$\varphi_c \approx 2i^{3/2}\left(\frac{\rho_w}{\rho_b}\right)\left(\frac{2}{\pi}\right)^{1/2} r^{-5/2} \times \left[m_{\ell_b} k_b^{-1/2} e^{-ik_b r} - \sum_1^{\ell_b-1} (m_{\ell+1}-m_\ell)\, k_\ell^{-1/2} e^{-ik_\ell r}\right] \quad , \tag{B13}$$

which is Eq. 42.

Note: Part of the analysis here and in Section V depends on the assumption that $f(k)=M|k|$ at sufficiently small real or imaginary k. Near k=0, β_1 is nearly equal to k_w and β_2, to k_b. The denominator of f(k) (Eq. 43) can cause no trouble even if $\cos(\beta_1 H)$ or $\sin(\beta_1 H)$ should vanish; condition 2 of Section VI is not met. However, $\sin(\beta_1 d)$, $\sin(\beta_1 z)$, or both might vanish at k=0. We outline the analysis for vanishing $\sin(\beta_1 d)$.

With $k^2 \ll k_w^2$, whether k is real or imaginary, Eq. 14 yields

$$\beta_1 d \approx k_w d - \frac{k^2 d}{(2k_w)} \quad . \tag{B14}$$

The assumption is that $k_w d$ is an integral multiple of π; the consequence is that

$$\sin(\beta_1 d) \approx \pm \sin\left(\frac{k^2 d}{2k_w}\right) \approx \pm\left(\frac{k^2 d}{2k_w}\right) \quad . \tag{B15}$$

Therefore $f(k)$ is approximately $M'k^3$, with M' a constant. The integrals corresponding to those of Eqs. 34 and 35, $r^{-4}\int (kr)^3 H_o^{(2)}(kr)d(kr)$, are known forms [B5,11] yielding Hankel functions multiplied by positive powers of k and negative powers of r. In addition, both integrals, one for real and one for imaginary k, have terms $\pm 8iM'/\pi r^4$ with opposite signs. As in Eqs. 34 and 35, these two terms--the only ones independent of k--cancel during integration "around the corner" at k=0. The surviving result, as in Eqs. 34 and 35, vanishes as $|k| \to 0$.

If both $\sin(\beta_1 d)$ and $\sin(\beta_1 z)$ vanish at k=0, the pertinent integrals contain a factor k^5. They can be evaluated by two applications of Ref. B5 and one of Ref. 11. The net results are much the same: two terms independent of k cancel each other. The remaining terms vanish as $|k| \to 0$.

REFERENCES AND NOTES

1. C. L. Pekeris, Geol. Soc. Am. Mem. 27 (1948).

2. W. M. Ewing, W. S. Jardetzky, and F. Press, Elastic Waves in Layered Media (McGraw-Hill Book Co., New York, 1957), pp. 126-142.

3. D. C. Stickler, J. Acoust. Soc. Am. 57, 856-861 (1975).

4. C. L. Bartberger and L. Ackler, "Normal Mode Solutions and Computer Programs for Underwater Sound Propagation; Part I--Two-Layer and Three-Layer Programs," Naval Air Dev. Cent. Rept. No. NADC-72001-AE (4 April 1973).

5. C. L. Bartberger, J. Acoust. Soc. Am. 55, S33(A) (1974).

6. F. M. Labianca, J. Acoust. Soc. Am. 53, 1137-1147 (1973).

7. C. T. Tindle and K. M. Guthrie, "Virtual Modes and the Surface Boundary Condition in Underwater Acoustics." Submitted for publication in J. Sound Vib. (private communication).

8. M. A. Biot and I. Tolstoy, J. Acoust. Soc. Am. 29, 381-391 (1957).

9. A. O. Williams, Jr., J. Acoust. Soc. Am. 59, 1175-1179 (1976).

10. A. O. Williams, Jr., J. Acoust. Soc. Am. 59, 62-68 (1976).

11. M. Abramowitz and I. A. Stegun, eds., Handbook of Mathematical Functions (National Bureau of Standards, Washington, D.C., 1965), Eqs. 9.1.4, 11.3.20, 11.3.24.

12. See Ref. 2, p. 142.

13. After Ref. 7 was received, its analytical fit to a resonance [in the form $A/(1+B\epsilon^2)$] was compared with our Eq. 45, which is purely empirical. The fitting equation of Ref. 7 was definitely better but not enough so to warrant the repeating of the calculations leading to our Fig. 2.

14. D. C. Stickler kindly provided full page versions of his Figs. 8 through 11, thereby facilitating our calculations.

15. L. M. Brekhovskikh, Waves in Layered Media (Academic Press, New York, 1960), pp. 379-382.

16. N. N. Voitovich and A. D. Shatrov, Sov. Phys. Acoust. 18, 434-438 (1973).

17. A. O. Williams, Jr., J. Acoust. Soc. Am. 32, 363-371 (1960).

18. See Ref. 11, Sec. 7.3, Eqs. 1, 2, 9, 10, 20; Sec. 7.4, Eqs. 22 and 23.

B1. See Ref. 11, Eq. 11.17.

B2. See Ref. 11, pp. 495-500.

B3. See Ref. 11, Eqs. 12.1.30, 31.

B4. See Ref. 11, Eq. 9.1.16.

B5. G. N. Watson, Theory of Bessel Functions (Cambridge University Press, 1966, 2nd edit.), Eq. 5.1(4).